Research Article

Towards Stable Porous Crystalline Phases of Molecular Belts

Marco Bernabei*, Raul Perez Soto, Ismael Gómez García, and Maciej Haranczyk*

[a] IMDEA Materials Institute, C/Eric Kandel 2, 28906 - Getafe, Madrid, Spain

[b] Universidad Carlos III de Madrid, Avda. Universidad 30, 28911 Leganés, Spain

* Corresponding author

Crystal Engineering Communications, 2017, 19, 6932-6935

Abstract: Porous molecular crystals are rare. They can sometimes be obtained by crystallization from a specially selected solvent, in which case they may lose their porosity upon solvent removal. By using an example of a molecular belt that suffered from this phenomenon, we demonstrate a structure modification that renders the molecule into a stable supramolecular nanotube crystal.

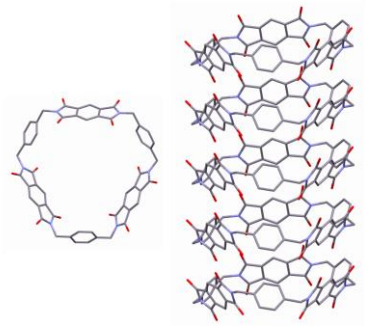

1. Full work presentation

Molecular belts, i.e. organic macrocycles with permanent cavities accessible from two opposing windows, have drawn researchers' attention over the last 20 years for their ability to spontaneously assemble into supramolecular nanotubes with potential applications in molecular or ion transport, separations, storage, encapsulation, molecular recognition as well as chemical reaction vessels[1].

Molecular belts can stack into tubular structures by the means of hydrogen bonds, π-interactions, chalcogen and halogen directional interactions[2]. However, the same intermolecular interaction may drive the molecular assembly towards more dense and non-porous structures. It is often up to nuances in the molecular geometries to favor one form over another, or alternatively allow for polymorphism. Crystal engineering techniques are used to steer crystallization towards porous phases, i.e. solvent molecules can stabilize the porous structure by occupying the voids[3,16]. In many cases, however, later removal of the solvent from the crystal will perturb the thermodynamic stability of the crystal phase, thus inducing a structural transition to either a denser phase or to an amorphous phase, thus affecting the porosity of the material. Indeed, obtaining stable porous crystals made of intrinsically porous molecules is considered a great challenge[3].

The outlined scenario applies to the pyromellitic diimide-based macrocycle molecule, denoted M1, presented in Figure 7-1. Molecule M1 was synthesized for the first time by Iwanaga and co-corkers in 2006 as a structural unit aimed at forming molecular tubes in the crystalline phase for the inclusion of organic molecules[2e,2f]. In their work, the authors were able, by tuning the solvent used for crystallization, to form several guest-host crystal complexes in which the host molecules M1 regularly stack to form tubular structures (left panel in Figure 7-2). Solvent molecules are entrapped inside and in between the tubular

cavities and in between thus promoting the assembly of the molecular nanotubes with coaxial channels. The host(i.e. M1)-guest crystal complexes were deposited in the Cambridge Structure Database (CSD) under the following IDs: YELKUW, YELLAD, EHETIV depending on the solvent used[4]. We characterized the porosity of the aforementioned experimental structure after manually removing the solvent molecules. The corresponding Pore Limiting Diameter (PLD) and the Largest Cavity Diameter (LCD) was calculated using our Zeo++ program[5]. The pairs (PLD,LCD) for YELKUW, YELLAD and EHETIV are respectively: (4.95Å, 6.49Å), (6.52Å, 7.86Å) and (5.09Å, 7.85Å). We note that the LCD values are close to the value of the pore diameter of the lowest energy conformer of M1 in the gas phase[6] (Figure 7-1).

To underline the role of the solvent as a 'glue' stabilizing the nanotube-like supramolecular assembly in the crystal phase, we studied the thermal stability of the above mentioned desolvated structures by performing molecular dynamic (MD) simulations at T=300K and P=1atm. MD simulations were performed with the GROMACS package[10] and the molecules modeled with the OPLS_2005 force field, which has been successfully applied to investigate the thermal stability of porous molecular materials with similar chemistry[11]. At the end of a 1 ns MD simulation we observed that the original crystal symmetry was completely destroyed, and that the system transitioned to a denser phase with a severe disruption of the 1-dimentional stacking order (Figure 7-2 right panel). A similar phenomenology was also experimentally observed for the supramolecular xerogel phase obtained from a hot solution of M1 in N,N-dimethylaniniline[2e]. After solvent removal by drying in vacuum, the height of the peaks in the XRD spectrum corresponding to the tubular stacking, dramatically decreased and broadened thus indicating a partial loss of the molecular stacking order.

To further investigate the stability of desolvated crystal phases of M1 and their corresponding porosity properties, we performed a computational study by means of

crystal structure prediction (CSP) calculations. Recent experiments demonstrated that extrinsic porosity of organic cages materials can be enhanced by fine tuning the vertex functionality of the cages[12]. On the other hand, the presence of peripheral groups on the perimeter of the cage windows can affect the porosity properties of the material by partially blocking the accessible windows and preventing the formation of guest-accessible channels connecting the molecular pores. For this reason, we included in our CSP study a tuned version of M1, denoted M2 (Figure 7-1 right panel), in which the methoxy side groups where removed from the molecule's benzene rings. Side-by-side comparison of M1 and M2 allows assessment of the role of side groups on the phase stability and porosity properties of the material.

CSP methods have been successfully applied to guide the experimental discovery of porous molecular crystals with enhanced porosity and gas selectivity properties[11,13]. CSP results are typically presented as energy landscape, i.e. plot of predicted lattice energy w.r.t structure density for each predicted phase. The set of structures with the lowest predicted energy at a certain density constitutes what is called the leading-edge of the energy landscape. Experimental accessible structures are often identified in this region of the landscape[11,14]. It is not unusual for porous molecular materials to observe low density polymorphs within an energy range of up to 50kJ mol^{-1} [11,13] from the lowest predicted structure and a relative energy difference that can exceed 20kJ mol^{-1} [14]. Our CSP approach performs a static lattice energy minimization of previously random generated trial solvent-free structures in the most common space groups (P21/c, P-1, P212121, P21, Pbca, C2/c, Pna21, Cc, Pca21, C2,P1, Pbcn, Pc) which account for 90% of the observed organic molecular crystals with one molecule in the asymmetric cell. Calculations involve the UPACK[15] (Utrecht Crystal Package) program suite and the OPLS_2005 force field to model the lattice energy. Geometrically equivalent structures are grouped after the minimization by means of a clustering algorithm based on interatomic distances. Even though our method only

involves one molecule per asymmetric cell and does not include solvent, it was able to predict the solvent induced polymorphism observed experimentally for organic porous cage molecules[9]. The porosity of the predicted structures was characterized in terms of PLD and LCD by our Zeo++ program[5]. The obtained energy landscapes for M1 and M2 are presented in Figure 7-3.

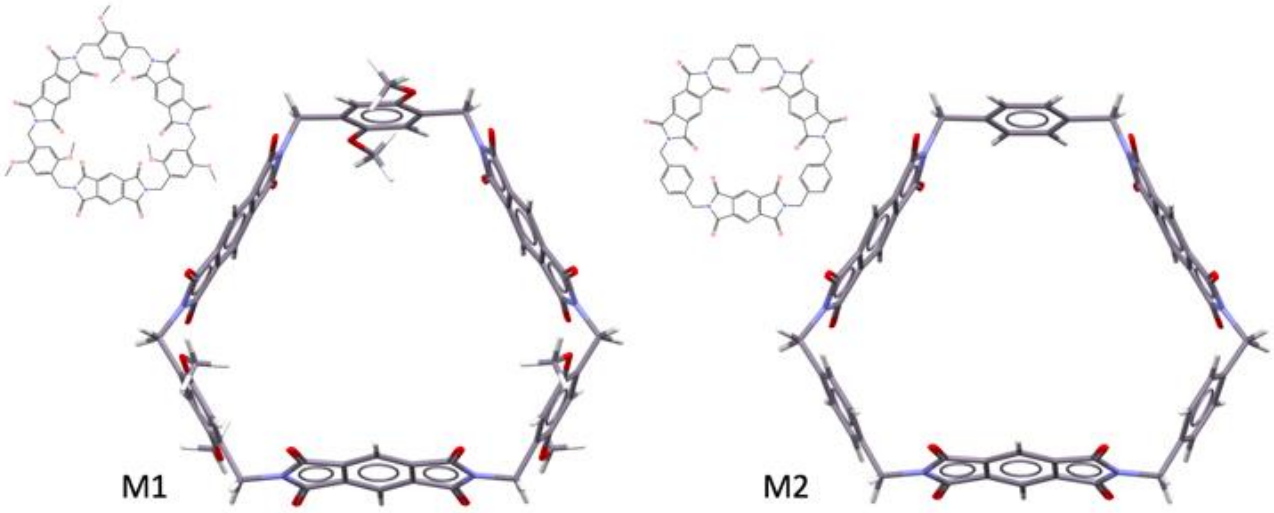

Figure 7-1. Pytomellitic diimide-based macrocycles studied in this work. Grey, blue, red and white represent carbons, nitrogen, oxygen and hydrogen atoms, respectively. The pore diameters of the lowest energy conformers of M1 and M2 measured with our tool are 8.72Å and 8.64Å respectively.

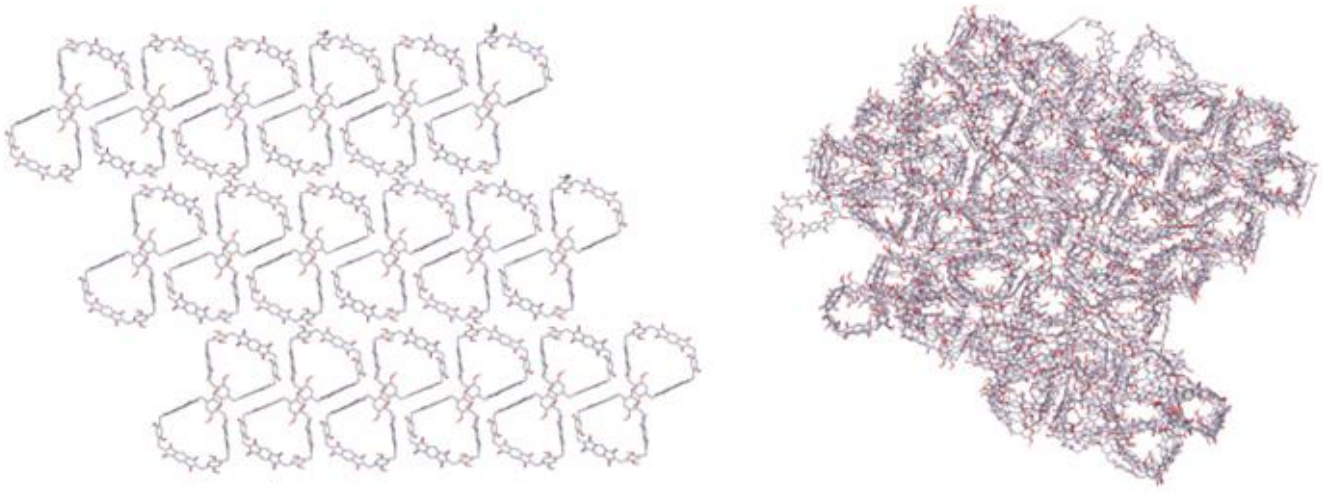

Figure 7-2. Snapshots of of YELKUW crystal structure at the beginning (left panel) and at the end (right panel) of a 1 ns length MD simulation. The simulation involved a 3x5x3 supercell with 180 porous molecules (no solvent) run at T = 300 K and P = 1atm.

The crystal energy landscape for M1 (top panel in Figure 7-3) resembles the typical one observed for organic molecules. The leading-edge of the landscape as a function of density decreases almost monotonically and the majority of the predicted structures are non-porous. Phases corresponding to 1D supramolecular nanotubes locate in the upper-left region of the plot, with the relative lattice energy above 40kJ/mol, which is in line with experimental observations of lack of stability upon solvent removal. In contrast to M1, the energy-density plot of M2 (bottom panel in Figure 7-3) shows a very different features. One can clearly distinguish two branches, a low density one (< 1.2 g cm^{-3}) and a high density (> 1.2 g cm^{-3}) one. A more detailed inspection of the energy-density plot reveals that several low-density structures, with density around 1.15 g cm^{-3}, are predicted in the low energy region of the landscape, i.e. ca. 20 kJ mol^{-1} with respect to the lowest energy phase.

By inspecting the PLDs of the structures included in the energy landscapes in Figure 7-3 we defined the α-phase and the β-phase as the lowest energy predicted structures with PLD larger than the 2.32 Å and 4.95 Å, respectively. The first threshold at 2.32 Å

represents the PLD of the experimental polymorph CC1-β of the imine cage CC1, which is porous to H_2.[16] The second threshold value of 4.95 Å corresponds to the PLD of the YELKUW experimental structure of M1 without solvent. Structures with PLD above the latter threshold are expected to feature 1D tubular channel due to stacking of the molecules. The predicted α-phases for M1 and M2 both lie in the leading-edge of the high density region of the landscape (labeled and indicated in Figure 7-3). The corresponding value of the LCD are less than half of the pore diameter of individual molecules of M1(M2) thus suggesting the lack of parallel stacking of the molecules as confirmed by visual inspection of the structures (Figure 7-4 top panel).

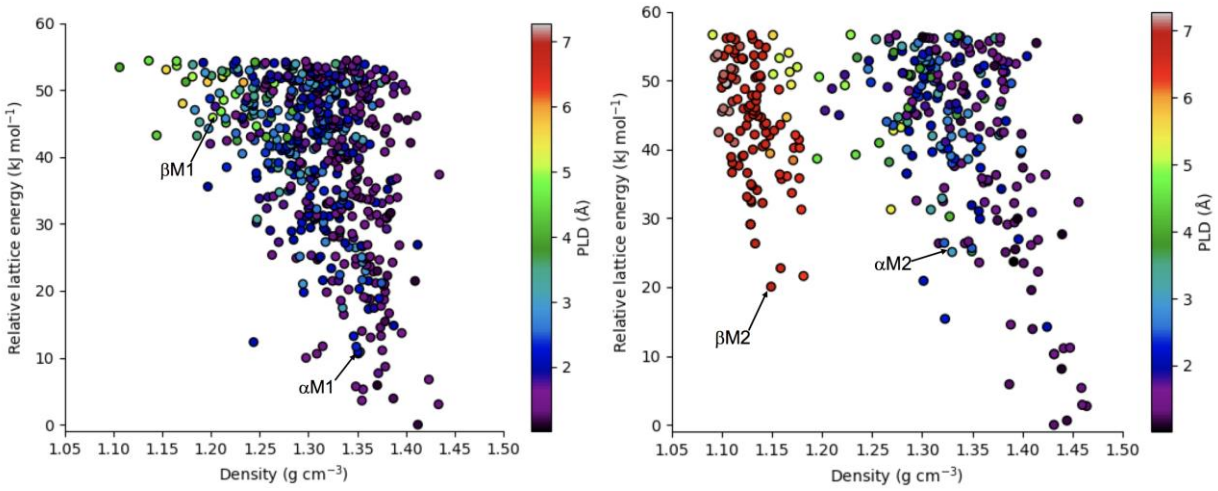

Figure 7-3. Energy landscape of molecule M1 (top) and M2(bottom). The α-phases and the β-phases are labeled and indicated. Each symbol is color coded according to the PLD value of the corresponding crystal structure.

These findings agree with the results of the MD simulations discussed above. The predicted low-density β-phases (Figure 7-4 bottom panel) also belong to the leading-edge of the landscape. In particular, the β-phase of M2 represents the lowest energy minimum in

the low-density branch of the landscape. Closer inspection confirms that 33% of the predicted structures within $\Delta E < 50$ kJ mol^{-1} lie in the low density branch (density <1.2 g cm^{-3}), with a PLD larger than 4.95 Å and 1-dimensional channels formed by parallel stacked M2 molecules. On the other hand, the β-phase of M1 lies 45.88 kJ mol^{-1} above the energy of the global minimum and that only 0.6% of the predicted structures with $\Delta E < 50$ kJ mol^{-1} features a PLD larger than the threshold of 4.95 Å. The presence of the methoxy groups in M1 frustrate the parallel stacking thus favoring a higher density packing with interpenetration of the molecules.

The thermal stability of both α and β polymorphs of M1 and M2 was assessed by performing MD simulations at 300K and 1atm. Visual inspection of the snapshots at the beginning and the end of 1 ns second simulations confirmed that the β-structures are stable and maintain their spatial order with a decrease of the density of approximately 2% due to temperature effects.

e

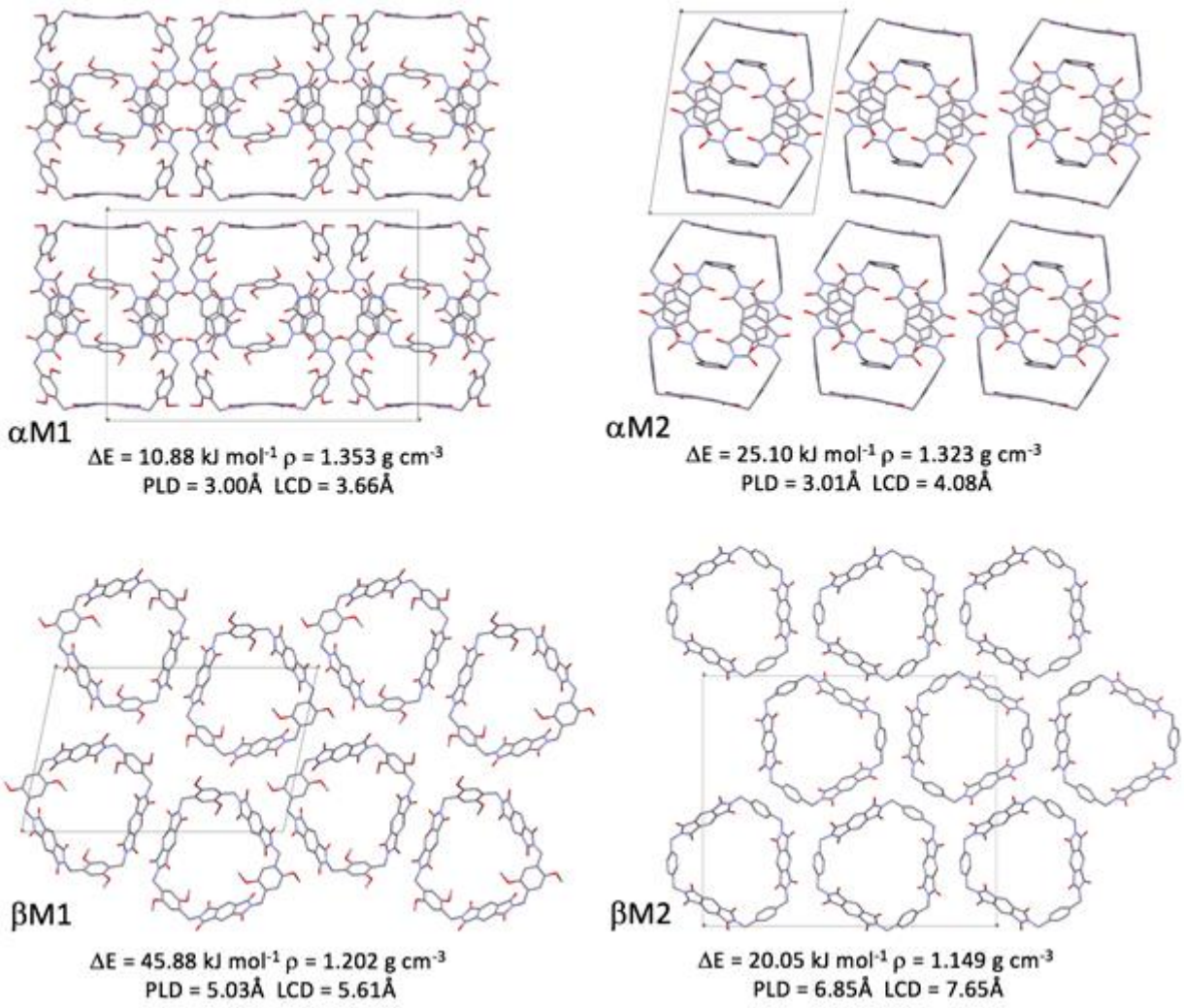

Figure 7-4. Predicted lowest energy crystalline structures for M1-M2 with PLD above the threshold value of 2.32Å (α phase) and 4.95Å (β phase), respectively.

In conclusion, we have employed a CSP approach to study the energy landscapes of two molecular belt molecules, which are expected to form porous crystal structures featuring 1D coaxial channels. The analysis of the energy landscape of M1, together with a MD simulation, confirms the previous experimental observation that porous M1 phases lack long range tubular order upon solvent removal. However, we demonstrated that a version of M1, denoted M2, which lacks the methoxy groups of its structure, may form stable phases with 1D tubular channels. We expect that this phase can be experimentally obtained through a routine crystal engineering procedures. Furthermore, our hybrid CSP/MD approach can help to assess the stability of other experimentally accessible porous molecular crystals that feature solvent molecules in the cavities and assist experimentalists with tuning the intramolecular architecture of a molecule in order to obtain more stable and porous crystalline phases.

2. Notes and References

Acknowledgements

Authors acknowledge support from the Spanish Ministry of Economy and Competitiveness (RYC-2013-13949) and resources of the National Energy Research Scientific Computing Center, a DOE Office of Science User Facility supported by the Office of Science of the U.S. Department of Energy under Contract No. DE-AC02-05CH11231.

Keywords: macrocycles • supramolecular nanotubes • crystal structure prediction • porous materials • molecular dynamic simulations

Bibliography

1. A) H. Sakamoto, T. Fujimori, X. Li, K. Kaneko, K. Kan, N. Ozaki, Y. Hijikata, S. Irle, K. Itami. *Chemical Science* **2016**, *7*, 4204-4210; b) T. A. Hilder, D. Gordon, S. H. Chung, *Nanomedicine: NBM* **2011**, *7*, 702-709; c) N. Kameta, M .Matsuda, T. Shimizu, *ACS Nano* **2012**, *6*, 5249-5258; d) H. Cao, P. Duan, X. Zhu, J. Jang, M. Liu, *Chem. Eur. J.* **2012**, *18*, 5546-5550; T. Okazaki, K. Suenaga, K. Hirahara, S. Bandow, S. IiJima, H. Shinoahara, *J. Am. Chem. Soc.* **2001**, *123*, 9673-9674; e) B. W. Smith, M. Monthioux, D. E. Luzzi, *Nature* **1998**, *396*, 323-324.

2. a)M. Tominaga, E. Takahashi, H. Ukai, K. Ohara, T. Itoh, K. Yamaguchi, Organic Letters 2017, 19, 1508-1511;b) R. Gleiter, D. B. Werz, B. J. Rash, Chem Eur. J. 2003, 9, 2676-2683;c) A. Bauza, A. Frontera, Phys. Chem. Chem. Phys. 2017, 19, 12936-12941;d)I. Hisaki, S. Nakagawa, N. Tohnai, M. Miyata, Angew. Chem. In. Ed. 2015, 54, 1-6;e) T. Nagasaki, A. Harano, Y. Fuchigami, E. Tanaka, S. Kidoaki, T. Okuda, T. Iwanaga, K. Goto, T. Shinmyosu, Angew. Chem. In. Ed. 2010, 49, 9676-9679;f) T. Iwanaga, R. Nakamoto, M. Yasutake, H. Takemura, K. Sako, T. Shinmyosu, Angew. Chem. In. Ed. 2006, 45, 3643-3647.;g)Z. Liu, G. Liu, Y. Wu, D. Cao, J. Sun, S. T. Schneebeli, M. S. Nassar, C A. Mirkin, J. F. Stoddart, J. Am. Chem. Soc. 2014, 136, 16651-16660;h) H. Sakamoto, T. Fujimori, X. Li, K. Kaneko, K. Kan, N. Ozaki, Y. Hijikata, S. Irle, K. Itami, Chem. Sci. . 2016, 7, 4204-4210.

3. T. Hassell, A. I. Cooper, Nature Materials 2016, 543,657-664

4. Structures YELKUW and YELLAD were experimentally obtained[2f] by recrystallization of M1 from a mixture of CH2Cl2/p-xylene and CH2Cl2/toluene, respectively. Structure EHETIV was obtained[2e] by recrystallization of M1 from a mixture of C2H2Cl4/N,N-dimethylaniline.

5. T. F. Williams, C. H. Rycroft, M. Kazi, J. C. Meza, M. Haranczyk, Mesoporous Materials 2012, 149, 134-141; www.zeoplusplus.org accessed July 13th, 2007.

6. Low energy conformer search was performed by using the Schrodinger's MacroModel tools[7]with the OPLS_2005 force field[8]. Molecular pore diameters were measured with our pore detection tool[9].

7. Materials Science Suite 2017-2, Schrödinger, LLC, New York, NY, 2017.

8. J. L., Banks, H. S. Beard, Y. Cao, A. E. Cho, W. Damm, R. Farid, A. K. Fetls, T. A. Halgren, D. T. Mainz, J. R. Maple, R. Murphy, D. M. Philipp, M. P. Repasky, L. Y. Zhang, B. J. Berne, R. A. Friesner, E. Gallicchio, R. M. Levy, J. Comp. Chem. 2005, 26,1752-1780.

9. I. Gomez Garcia, M. Bernabei, R. Perez Soto, M. Haranczyk, Crystal Growth & Design. Submitted.

10. D. Van Der Spoel, E. Lindhal, B. Hess, G. Groenho, A. E. Mark, H. J. C. Berendsen, J. Comp. Chem. 2005, 26, 1701-1718.

11. A. Pulido, L. Chen, T. Kaczorowski, D. Holden, M. A. Little, S. Y. Chong, B. J. Slater, D. P. McMahon, B. Bonillo, C. J. Stackhouse, A. Stephenson, C. M. Kane, R. Clowes, T. Hassell, A. I. Cooper, G. M. Day, Nature 2016, 543,657-664.

12. M. J. Bojdys, M. E. Briggs, J. T. A. Jones, D. J. Adams, S. Y. Chong, M. Schmidtmann, A. I. Cooper, J. Am. Chem. Soc. 2011, 133, 16566-16571.

13. E. O. Pyzer-Knapp, H. P. G. Thompson, F. Schiffmann, K. E. Jelfs, S. Y. Chong, M. A. Little, A. I. Cooper, G. M. Day. Chem. Sci. 2014, 5, 2235−2245.

14. A. J. Cruz-Cabeza, G. M. Day, W. Jones, Chem. Eur. J. 2009, 15, 13033-13040.

15. B. P. Van Eijck, J. Krooj, Acta Cryst. B 2004, 56, 535-542.

16. J. T. A. Jones, D. Holden, T. Mitra, T. Hasell, D. J. Adamas, K. E. Jelfs, A. Trewin, D. J. Willock, G. M. Day, J. Bacsa, A. Steiner, A. I. Cooper, J. Angew. Chem. 2011, 123, 775-779.

3. Supporting information

3.1 MD simulations to assess the thermal stability of desolvated crystal structures.

In order to investigate the thermal stability of the experimental crystal structures of M1(CSD Refcodes: YELKUW, YELLAD, EHETIV) we first manually removed the solvent molecules from the the corresponding CIF file downloaded from Cambridge Structure Database (CSD) to create a fully desolvated structure. In figure S1 we depict a projection along the b-axis of the filled unit cell of YELKUW including solvent (left panel) andwithout solvent (right panel).The desolvated structures were then used to build a supercell (see Fig. S2 top-leftpanel as an example for the desolvated YELKUW structure) containing 180 molecules and that constituted the starting point of the molecular dynamic (MD) simulations withperiodic boundary conditions carried out with the GROMACS package. A time step of 1.5 fs was used and the Berendsen thermostat and barostat were employed to keep the system at P=1atm and T=300K. The OPLS_2005 force field was employed to model both inter and intramolecular interactions. At the end of a 1ns length simulation we visually inspected the last snapshot and we observed that the system lost the initial symmetry and evolved to a denser phase, with an increase of about 15 % in density and a decrease of about 50% in the value of the PLD. The same simulation protocol involving the construction of a supercell (Fig. S2bottom panel) and the subsequent MD simulation was also applied to assess the thermal stability of the crystal phases αM1, αM2, βM1 and βM2 (Figure 3 in the main text)predicted by our CSP approach described in the main text and section

As an example, in the bottom panel of figure S2 we depict a 4x5x4 supercell (180 molecules) of the predicted βM1 structure (see section S5 for the corresponding crystallographic information) at the beginning (left) an at the end (right) of a 1ns MD

simulation at P=1atm and T=300K. Simulations details are described above. In this case, at the end of the simulation run we observe that the system still conserves the initial symmetry, the density decreases of a 2.5 % due to thermal effects and that the value of the PLD barely changes.

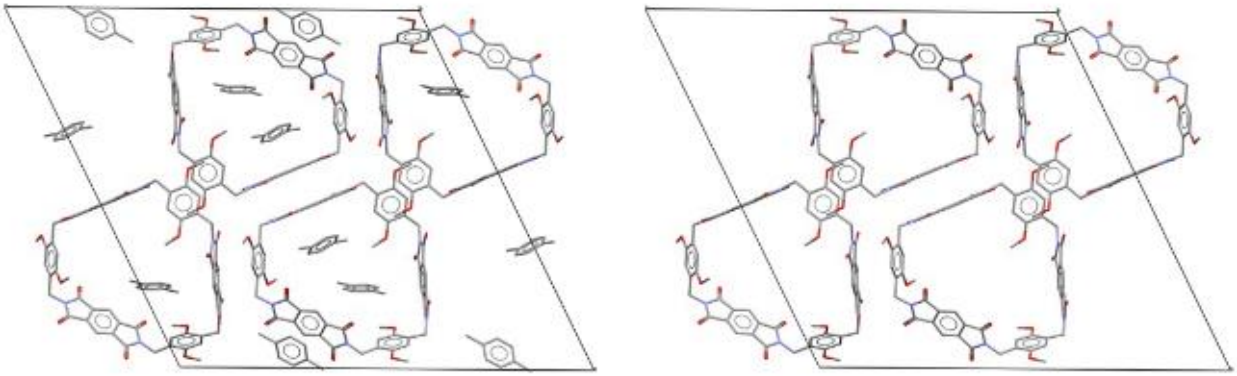

Figure 7-S1. Projection along the b-axis of the filled unit cell of the experimental structure YELKUW including solvent (left panel) and without solvent (right panel). Hydrogen atoms are not included for clarity

3.2 Single molecule conformational analysis

The coordinates of molecule M1 and M2 where first generated with the Schrodinger's tool LigPrep (1), which is a robust collection of tools designed to prepare high quality, all-atom 3D structures for molecules of up to 900 atoms, starting with SMILES sequences, 2D or 3D structures in SD (.sdf) or Maestro (.mae) format. The molecules generated with LigPrep where submitted to a conformational search routine that performs an initial cycle of several short MD simulated annealing runs followed by a conformational sampling by means of the LargeLow-Mode sampling technique implemented in the Schrodinguer's MacroModel suite (1). The conformational search uses the OPLS_2005 force field (FF) to model intramolecular degrees of freedom and non-bonded interactions. The OPLS_2005 FF is an enhanced version of the original OPLS force field, and is developed by the Schrodinger

company to provide a bigger coverage of organic functionality. In particular, intramolecular parameters have been fit to reproduce the conformational energies derived at a higher level of quantum theory for a large set of organic molecules.

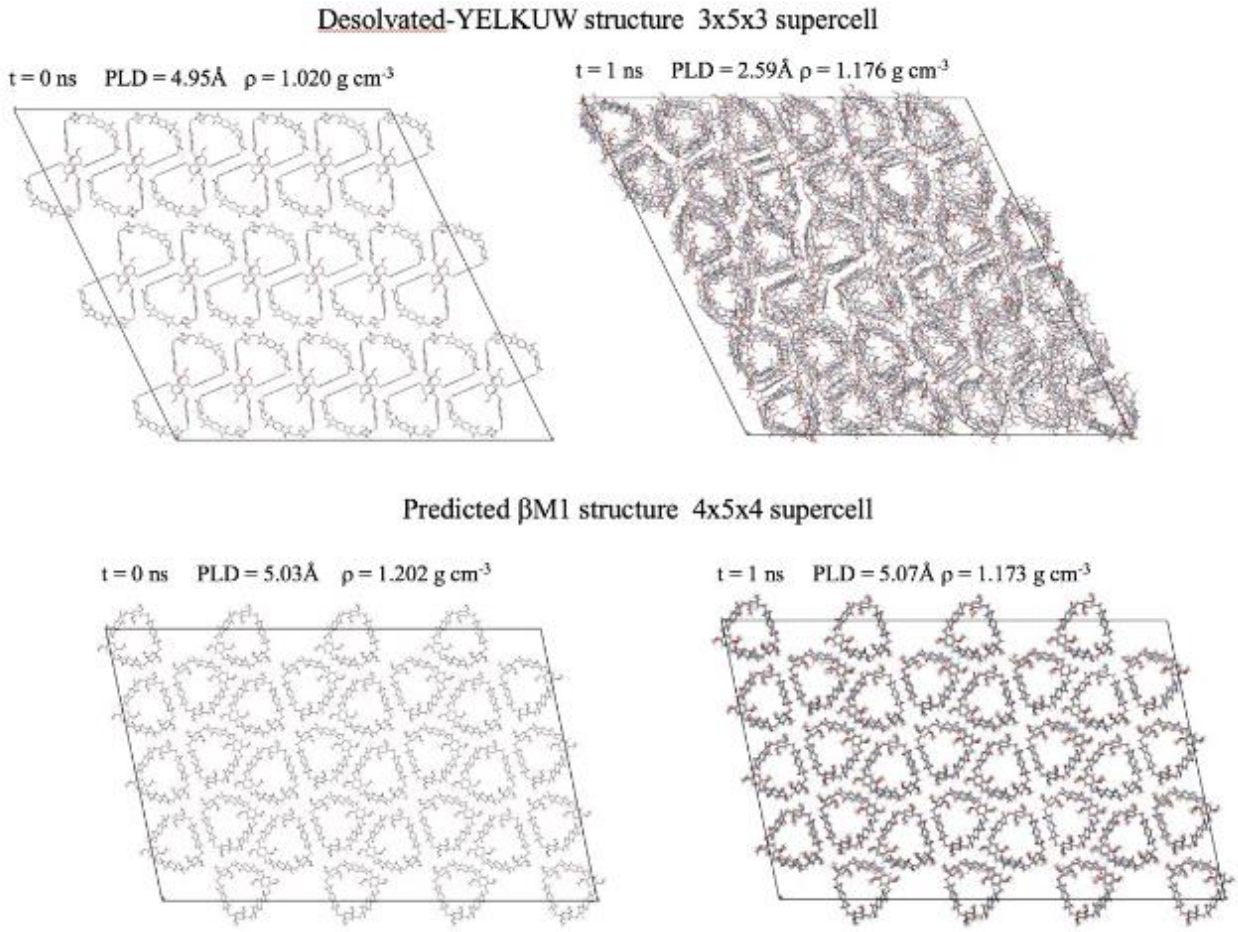

Figure 7-S2. Top panel: Projection along the b-axis of a 3x5x3 supercell of the manually desolvated experimental YELKUW structure at the beginning (left) an at the end (right) of a 1ns MD simulation. Bottom panel: Projection along the b-axis of a 4x5x4 supercell of the predicted ßM1 structure at the beginning (left) an at the end (right) of a 1ns MD simulation.

To assess the quality of the intramolecular modeling provided by the OPLS_2005 force field the generated conformers of M1 and M2 within an energy range of 30kJ/molfrom the lowest energy one where subsequently optimized with DFT-B3LYP/6-31G* calculations performed with the Schrodinger's Jaguar ab-intio package (1). In figure S3 we depict the comparison of the OPLS_2005 conformers (red lines) to the DFT-optimized ones (blue

lines) and we quantify the structural differences by measuring the Root-Mean-Square-Deviation (RMSD) of atomic positions for heavy atoms. The agreement is good for both M1 and M2 low energy and high energy conformers.

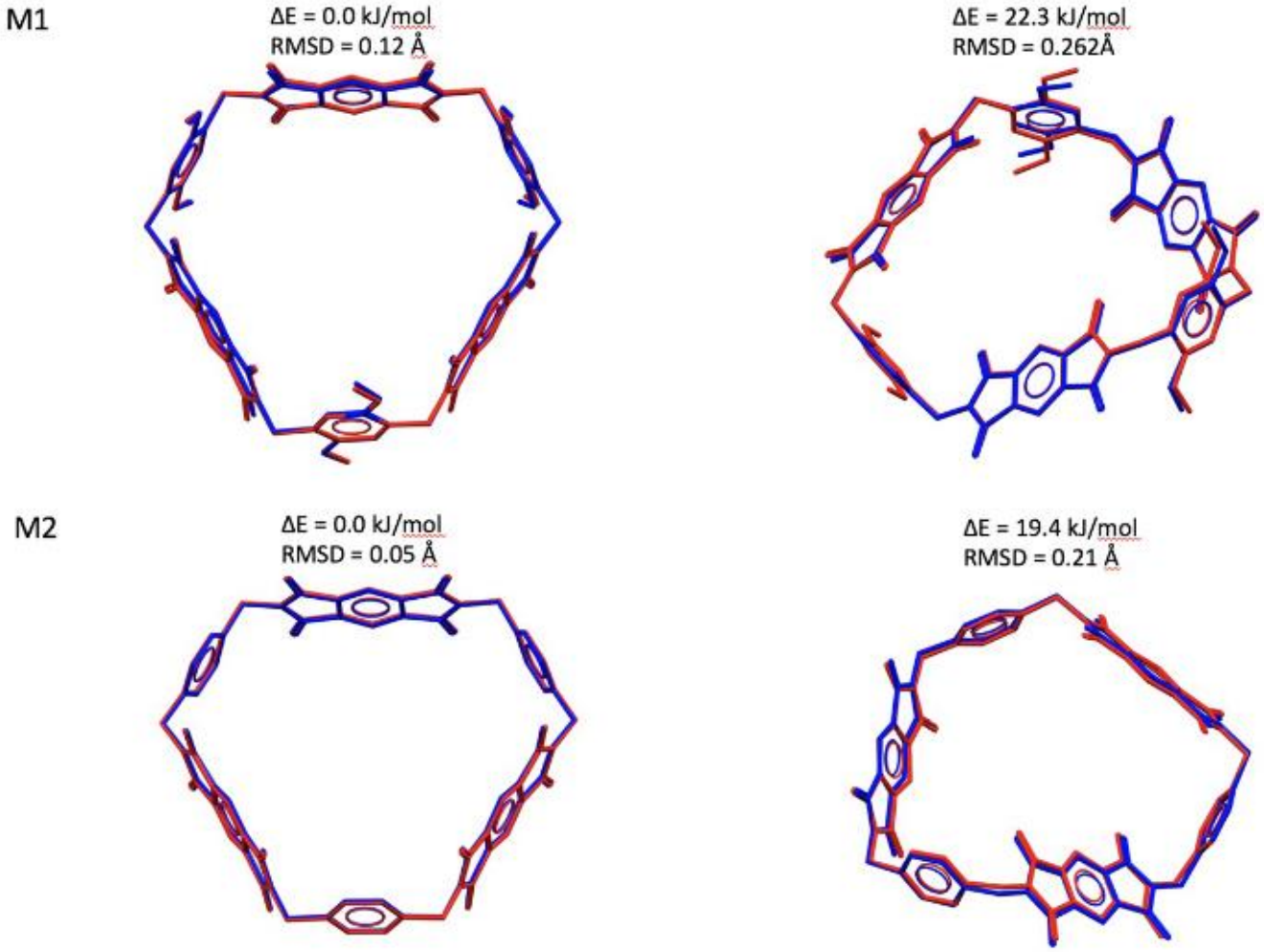

Figure S3. Overlay of the molecular geometries of the OPLS_2005 conformers (blue) and the corresponding DFT-B3LYP/6-31G* optimised ones. The values of the Root-Mean-Square deviation of atomic position show good agreement.

Finally, we note that the diameter of the cavity of both lowest energy conformers(ΔE= 0.0 kJ/mol) of M1 and M2, measured with our pore detection algorithm described in Ref. 2, takes the value of 8.62Å and 8.74Å. The intrinsic molecular pores of the high energy conformers(ΔE= 22.3 kJ/mol for M1 and ΔE = 19.4 kJ/mol for M2) are smaller though, their diameters take the values of 6.2Å and 6.3Å for M1 and M2, respectively. The

molecular geometry of the lowest energy conformer where adopted to start the initial random search at the beginning of the Crystal Structure Prediction procedure. See section S3 for further details. Further technical details about LigPrep, MacroModel conformational tool and our pore detection algorithm can be found in the ESI of Ref. 2.

3.3 Crystal structure prediction

Crystal structure prediction (CSP) calculations presented in this work were performed using a random search technique implemented in the UPACK (Utrecht Crystal Package)program suite (3). UPACK provides hypothetical crystal structures by approximating the free energy of the crystal with a static lattice energy and minimizing it by using a molecular force field (FF). The latter is defined as the sum of an intermolecular potential, consisting of van der Waals and Coulomb terms, and a combination of intramolecular energy terms, which account for molecular flexibility. We employed the widely used transferable OPLS_2005 force field to model the lattice energy for the systems considered in this study. In the OPLS_2005-FF framework, the intermolecular potential energy is modeled as the sum of Lennard-Jones and Coulomb terms while intramolecular interaction includes stretching, bending and torsional terms. As stated above, static lattice energy minimization is at the core of the UPACK method for crystal structure prediction simulations. Energy minimization steps are normally performed by a combination of the steepest descendent method followed by a 4.

certain number of conjugated gradient minimization steps. Intermolecular interactions are truncated at a certain cut-off based on the charged groups distance and the Ewald summation method is employed for Coulomb and Lennard-Jones r-6 dispersion terms. A full CSP study with UPACK was carried out in three steps:

1. In the first step, we generated candidate structures (5000 are usually sufficient) by means of a random search method combined with a rough energy minimization (using a cut-of 8Å for intermolecular interactions). Initial structures are generated for a set of selected space groups with Z'=1 molecules in the asymmetric unit. The number of degrees of freedom for the random search comprehends up to 6 variables for the unit cell plus 6 degrees of freedom that describe global translation and rotation of the molecule in the unit cell. For molecules with rotatable bonds further degrees of freedom are considered during the random search to account for different molecular conformations. The total number of degrees of freedom, D, cannot be arbitrarily large for the random search method to be successful. Indeed, it was empirically noticed9that the random search method started to fail when the total number of random variables is around 20.

2. During this step, a minimization of the static lattice energy with a larger cut-off of 20.0Å w.r.t all the degrees of freedom was used to further refine the structures generated in Step 1.

3. Equivalent structures resulting from different initial orientations of Step 1 were grouped together by the means of a clustering algorithm based on interatomic radial distribution functions as implemented in UPACK. The final set of unique structures was finally ranked according to their lattice energy relative to the lowest minimum found.

Our aforementioned procedure was tested and validated by performing the CSP calculations for the well-known porous imine cage CC1. CC1 cage molecule is one of a series of porous organic shape-persistent cages with large internal cavities synthesized in the group of Prof. Cooper of University of Liverpool, UK. These molecules have been of

great interest especially for their capacity to tune porosity when exposed to different solvents (4). In our CSP validation study the two experimentally observed desolvated polymorphs CC1-α' (non-porous) and CC1-β'(H2selectively porous) were predicted in the leading-edge of the low energy region of the energy landscape. More details about our validation procedure can be found in the ESI of Ref. 2Motivated by the results for porous cage CC1, we decided to apply UPACK prediction procedure to study the porosity properties of the predicted structures for the molecules M1 and M2 introduced in the main text.

3.4 H-bond patterns in the βM2 predicted structure.

In the case of theβM2 crystal phase, the lack of methoxy groups in M2 (w.r.t M1)enables the formation of intra (blue dashed line in Fig. S4) and inter-molecular (red dashed line in Fig. S3) hydrogen bonds (HB) by pairing the acceptors oxygen atoms with the phenyl H donor atom. According to the following geometric definition an HB is formed if the distance H··O is less then 2.6 Å and the angle CH··O is larger than 90°(5,6)

3.5 Crystallographic information for the predicted structures αM1, βM1, αM2, βM2

Can be found online: http://www.rsc.org/suppdata/c7/ce/c7ce01679d/c7ce01679d5.pdf

3.6References

1. MaterialsScienceSuite2017-Schrödinger,LLC,NewYork,NY,2017.2
2. I.Gomez Garcia, M.Bernabei R.PerezSoto, M.Haranczyk, CrystalGrowth&Design. JustAcceptedManuscript.DOI:10.1021/acs.cgd.7b01095.3
3. VanEijck, B.P.;Krooj, J.ActaCryst. B2004,56,535.4

4. J.T.A.Jones, D.Holden, T.Mitra, T.Hasell, D.J.Adamas, K.E.Jelfs, A.Trewin, D.J.Willock, G.M.Day, J.Bacsa, A.Steiner, A.I.Cooper, J.Angew.Chem.2011,123,775.5

5. Vincent de Paul N.Nzikoand Steve Scheiner, J.Org.Chem. 2015,80,2356.6P.

6. D.Vaz, M.Nolasco, N.Fonseca, A.M.Amado, A.M.Amorinda Costa, V.Felix, M.G.B. Drew, B.J.Goodfellow, P.J.A.Ribeiro-Claro,Phys.Chem.Chem.Phys.2005,7,3027.